Estimation rates of permafrost degradation and their impact on ecosystems across Alaska

Sergey Marchenko[1], Kevin Bjella[2], Dmitry Nicolsky[1] & Vladimir Romanovsky[1]

[1]*Geophysical Institute, University of Alaska Fairbanks, Fairbanks, Alaska, United States*

[2]*U.S. Army Engineer Research and Development Center (ERDC), Cold Regions Research and Engineering Laboratory (CRREL), Fairbanks, Alaska, United States*

Abstract

The main goal of this research is to evaluate the vulnerability and behavior of permafrost under climate warming across the different ecosystems and surface conditions in respect of ecosystem stability, socio-economic impact, and to provide stakeholders with information for better understanding possible future environmental changes. We suggested the new version of the spatially distributed permafrost dynamics model (GIPL2-MPI), which is developed in the Geophysical Institute (GI), University of Alaska Fairbanks (UAF). This model is based on the ecosystem approach to simulate the permafrost dynamics, which we are discussing in this paper. The combined ground-based observations and numerical freeze/thaw modeling using climate-ecosystem-permafrost interactions allow us to understand the physical processes and mechanisms controlling permafrost physical state. It was attempting to predict the changes in permafrost conditions using output from two GCMs (NCAR-CCSM4 and GFDL-CM3) and Five-Model Average for the RCP-4.5 and RCP-8.5 scaled down to 1 by 1 km spatial resolution (https://uaf-snap.org) across entire Alaska. Our result shows that by the end of the current century widespread permafrost degradation could begin everywhere in Alaska southward of the Brooks Range as well as across some spots of the North Slope. The most significant changes in the upper layer (0.5–5.0 m) of ground could occur under the climate scenario provided by the GFDL-CM3 climate model, especially in areas with ice-rich permafrost.

1 Introduction

Recent observations indicate a warming of permafrost in many northern regions with a resulting degradation of ice-rich and carbon-rich permafrost. In the last 30–40 years, warming in permafrost temperatures observed in the Northern Hemisphere has resulted in the thawing of permafrost in natural, undisturbed conditions in areas both close to the southern and north boundary of the permafrost distribution. The impact of climate warming on permafrost and the potential of climate feedbacks resulting from permafrost thawing have recently received a great deal of attention. Most of the permafrost observatories in the Northern Hemisphere show substantial warming of permafrost since the 1980s (Biskarbon et al. 2019; Smith et al. 2010; Romanovsky et al. 2010). The magnitude of permafrost warming has varied with location but was typically from 0.5 to 3 °C. A more pronounced warming has been observed in cold permafrost in higher northern latitudes and a smaller increase in temperature was typical for the warmer permafrost (because latent heat). Permafrost temperatures were stable or even slightly cooling during the last several years in the lower northern latitudes.

A comprehensive system of permafrost observatories at Alaska was established in the late 1970s and early 1980s by the Geophysical Institute, University of Alaska Fairbanks along the Trans-Alaska Pipeline and at other locations in Alaska (Osterkamp 2005, 2008).

Permafrost extent and active layer depth are very important for the high-latitude temperature regimes and water cycle. Changes in the hydrologic cycle and soil temperature can have significant consequences for local people: degrading permafrost very often could lead to ecosystem changes and threatens to damage infrastructure. Understanding how the tightly coupled permafrost and hydrology will behave in a warming world is vitally important for local communities in Alaska and throughout the circumpolar North.

Alaska is warming very fast. Permafrost temperature has increased by 0.5 to 2 °C in Alaska during the last 30 to 35 years (e.g., Osterkamp 2007; Romanovsky et al. 2010; Smith et al. 2010). Therefore, there is an urgent need to develop a robust modeling tool for projecting changes associated with thawing permafrost in this region. Many important questions about present day and future ecosystems change can be answered with such tools. Even with all the uncertainty of future climate change projections this model will be useful in creating estimations of the range of future permafrost change in Alaska. Many of the proposed developments will be experimental in nature, with a final goal of providing society with robust expert assessments of changes that are important for infrastructure for several decades ahead.

In the discontinuous permafrost zone with ground temperatures near the freezing point, the presence of vegetation and organic soil layers strongly affect the ground thermal regime due to insulation effect. Shur and Jorgenson (2007) classified permafrost according to patterns of formation and degradation in relation to climate and ecosystems. They propose five main permafrost zones:

1) Climate-driven;
2) Climate-driven, ecosystem-modified;
3) Climate-driven, ecosystem protected;
4) Ecosystem-driven; and
5) Ecosystem-protected permafrost.

https://doi.org/10.52381/ICOP2024.231.1

Permafrost in each zone reacts differently to external disturbances. The permafrost types ‘climate-driven, ecosystem protected’, ‘ecosystem-driven’, and ‘ecosystem-protected’ are in a state of disequilibrium with the current climate; minimal disturbances have already caused widespread permafrost degradation (Jorgenson et al. 2008).

Recently, several permafrost models were developed for various regions (e.g., Gisnås et al. 2013; Westermann et al. 2013; Zhang et al. 2013; Fiddes et al. 2015). In many of the permafrost models, properties for the mineral and organic soil layers (Marchenko et al. 2008; Jafarov et al. 2012) or properties for the sediment and bedrock material (Westermann et al. 2013), or values of n factors and thermal properties of the ground material (Gisnås et al. 2013) produce a large number of distinct combinations of the input-data classes, the parameterization of which is a difficult task involving various assumptions and datasets. In some publications, the texture of mineral soils and other input parameters are used (Zhang et al. 2013) to reduce several input-data classes by considering 26 so-called ecosystem types.

In this manuscript, we consider the ecosystem types and group existing ground temperature observations across the ecosystem types. This grouping allows estimation of the soil properties using the data assimilation technique for each input-data class to Alaska. Justification of this approach is based on the analysis of spatial and temporal variability of near-surface ground temperatures measured across entire Alaska (Osterkamp and Jorgenson 2006; Osterkamp 2008; Romanovsky et al. 2008, 2010).

The modes of permafrost degradation are highly variable, and its topographic and ecological consequences depend on the interactions of slope positions, soil texture, hydrology, ice content, etc. However, it is still not clear how surface conditions could affect the hydrothermal dynamics of permafrost and active layer; how to determine these factors are most important in estimating for surface condition. Knowledge of processes affecting the vulnerability of permafrost in respect to ecosystems stability, infrastructures, and socio-economic impacts, provides stakeholders with information for better understanding the range of possible future changes, to help guide land management and decision-making.

2 Permafrost Dynamics Model GIPL2-MPI

To evaluate the vulnerability of permafrost under climate warming across entire Alaska in respect to ecosystems stability, infrastructure and socioeconomic we applied the physical process-based permafrost dynamics model developed in Geophysical Institute Permafrost Lab (GIPL) University of Alaska Fairbanks (Marchenko et al. 2008; Nicolsky et al. 2009; Jafarov et al. 2012).

In this research, we employ the transient permafrost dynamics model GIPL2-MPI, which simulates soil temperature dynamics and the depth of seasonal freezing and thawing by solving 1D non-linear heat equation with phase change using the finite difference method. The GIPL2-MPI model captures physical processes essential to robust and appropriate modeling of soil temperature dynamics, active layer thickness and talik development if so. Specifically, soil thermal properties are parameterized according to soil texture and organic matter. In this model, the process of soil freezing/thawing is occurring in accordance with the unfrozen water content and soil thermal properties, which are specific for each soil layer and for each geographical location. Additionally, GIPL2-MPI includes thermal insulation of the snow cover, and geothermal heating at the appropriately selected depth. The GIPL2-MPI model also incorporates an efficient algorithm to estimate soil thermal properties using in-situ temperature measurements in the active layer and in permafrost. This simplifies model calibration for specific sites. The conceptual representation of permafrost dynamics in the GIPL2-MPI Model could be expressed as:

- Numerical finite difference solution of heat diffusion,
- At least 100 m vertical computational domain (vertical depth’s grid), contains 128–256 vertical grid nodes,
- Moss insulation explicitly considered,
- Organic soil insulation explicitly considered,
- Snow insulation explicitly considered,
- Effect of unfrozen water on phase change explicitly considered,
- Thermal conductivity and heat capacity are the functions of soil moisture content, soil temperature, and unfrozen water.

3 Model validation and calibration

Different earth’s materials have varying thermal properties. The soil thermal conductivity and heat capacity vary within the different soil layers as well as during the thawing/freezing cycles and depend on the unfrozen water content that is a certain function of temperature. The method of obtaining these properties is based on numerical solution for a coefficient inverse problem and on minimization locally the misfit between measured and modeled temperatures by changing thermal properties along the direction of the steepest descent. The method used and its limitations are described in more detail elsewhere (Alifanov 1994; Alifanov et al. 1996; Tikhonov et al. 1996; Marchenko and Gorbunov 1997; Nicolsky, 2009).

For the initial model calibration, we used measured data from more than twenty shallow boreholes (1–1.5 m in depth) from across Alaska. These high-quality ground temperature measurements (precision generally at 0.01 °C) are available from the beginning of 1990s to present. Soil water content and snow depth measurements were also available at most of these boreholes for the different landscape settings for the initial model validation (Romanovsky and Osterkamp 1997; Osterkamp 2005; Romanovsky et al. 2010). The temperature measurements in the shallow holes performed with vertical spacing of 0.08–0.15 m. At most, of these sites, soil water content and snow depth also were recorded. In addition, more than 20 relatively deep boreholes, from 29 m to 100 m in depth, along the same transect were available for the model validation in terms of permafrost temperature profiles and permafrost thickness.

The developed approach attempts to addresses the problem of computing the ground temperature projections at the regional scale that is sufficient to gain some understanding how potential changes in the permafrost might affect ecosystems and impact the infrastructure under various climate scenarios. The developed parametrization of the ground thermal properties is obtained using a data assimilation technique (e.g., Marchenko and Gorbunov 1997; Nicolsky et al. 2009). The mean values for ALT are computed over the 1996–2022 period, while the MAGT values are computed over the period when the observations are available. Generally, the modeling results very well agree with observations (Figure 1).

The example of the reconstructed soil thermal properties is shown in Table 1. Some year-to-year differences between the modeled and observed annual cycles exist. However, in general, the modeled and observed ground temperature climatology agree well with each other. The error is typically less or close to 0.25 °C, except during the snowmelt season. The subsurface thermal properties input datasets were compiled using both the GIS environments and specially developed tools as well.

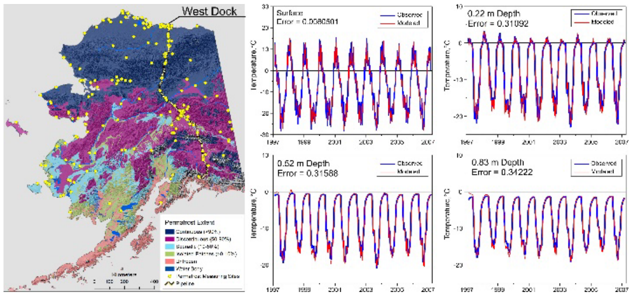

Figure 1. (Left) Map of measuring site locations (yellow dots), and (right) example of the GIPL2-MPI model calibration for the specific site west dock represents the north slope of alaska arctic tundra ecotype. The blue line is a measured data, and the red one is the GIPL2-MPI modeled.

4 Ecosystem Approach of Permafrost Dynamic Modeling

This research explores data on the ground thermal properties and surface conditions for the major ecotypes and deposits across Alaska, which were obtained using the ecosystem and vegetation maps, map of deposit types and ground ice as a source of a priory information (Figure 2) and the solution of the inverse problem as well (Alifanov 1994; Alifanov et al. 1996; Tikhonov et al. 1996; Marchenko and Gorbunov 1997; Nicolsky et al. 2009). For each ecosystem type the soil texture and thickness of the organic layer were parameterized according to field measurements and maps.

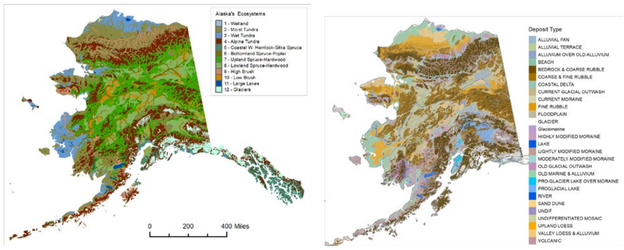

Figure 2. Ecosystem Map of Alaska (Geological Survey 1970) used for determination of properties for surface vegetation (left) and Map of Deposit Type of Alaska (Jorgenson et al. 2008) used for determination of soil thermal properties within the upper sub-surface soil layer (right).

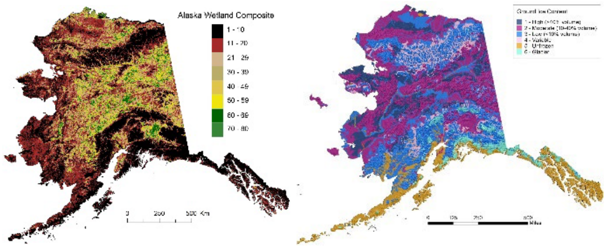

Figure 3. Alaska Wetland Composite map at 30 m spatial resolution (He et al. 2016) used for determination of soil water content (left). Excess ice volume in top 5 m based on surficial geology relationships (right). Variable ice associated with buried glacial ice (Jorgenson et al. 2008)

Table 1. The reconstructed ground thermal properties for sub-polar or polar soil type and moist and wet tundra (grassland-lichen-moss) ecosystem class at the North Slope Alaska (West Dock).

	Heat Capacity		Thermal Conductivity			
VWC (m^3/m^3)	Thawed ($J/m^3/K$)	Frozen ($J/m^3/K$)	Thawed (W/m*K)	Frozen (W/m*K)	Depth (m)	Layer matter (description)
0.694	1.72E+06	1.21E+06	0.242	0.895	0.0-0.12	moss
0.596	1.93E+06	1.51E+06	0.452	1.032	0.12-0.22	peat 1 (shallow organic, fibrous)
0.543	2.02E+06	1.65E+06	0.524	1.056	0.22-0.68	peat 2 (deep organic, amorphous)
0.456	2.54E+06	1.72E+06	1.023	1.516	0.68-5.68	mineral 1, silt
0.442	2.93E+06	2.23E+06	1.216	1.645	5.68-8.8	mineral 2, silt
0.426	3.43E+06	2.83E+06	1.424	1.849	8.8-48.5	mix of silt, gravel, sand, debris
0.384	3.63E+06	3.12E+06	1.832	2.214	48.5-52.0	gravel, coarse sand, debris
0.041	3.85E+06	3.46E+06	2.502	2.589	52.0-100	bedrock

We used the maps of surface vegetation, surficial geology, deposit types, primary soil texture, permafrost extent and ground ice volume. The map of ground ice distribution used for additional information to compile the initial soil ice/water content (Figure 3). Ground ice volumes were estimated for the upper 5 m of permafrost using terrain relationships established by Jorgenson et al. (2008) and our field data. Ground ice volume near the surface is higher in colder regions due to active ice-wedge formation and ice segregation in fine-grained deposits. Buried glacial ice in old or stagnant young moraines is included, but is irregularly distributed at this map scale.

5 Computational Domain and Climate Forcing

We defined the computational domain across Alaska with a spatial resolution of 1 by 1 km, which covered Alaska entirely except the small part of the Aleutian Islands. For computation this area consisted of 1,497,645 grid cells.

We prepared the SNAP dataset as a climate forcing to drive the GIPL2-MPI permafrost model. CMIP5/AR5 selected GCM's (https://uaf-snap.org/how-do-we-do-it) scaled down to 1 km spatial resolution were used to drive the GIPL2-MPI model. We used outputs for two operating separately GCMs GFDL-CM3 and NCAR-CCSM4 as well as for five-model average, and for two different greenhouse gas concentration trajectory RCP4.5 and RCP8.5.

The five-model average is the average model output from the top five models that best replicate historical climate in Alaska and the Arctic regions such as NCAR-CCSM4, GFDL-CM3, GISS-E2-R, IPSL-CM5A-LR, MRI-CGCM3 (Walsh et al. 2018). The five-model average is best for looking at general climate trends over time, as it smooths over the year-to-year and decade-to-decade variability. NCAR-CCSM4 and GFDL-CM3 are the best for the Alaska region for exploring climatic extremes or annual variability. Only individual models can provide that type of information.

RCP is a greenhouse gas concentration trajectory adopted by the IPCC (IPCC 2014). Four pathways were used for climate modeling and research for the IPCC fifth Assessment Report (AR5) in 2014. The pathways describe different climate futures, all of which are considered possible depending on the volume of greenhouse gases (GHG) emitted in the years to come. The RCPs—originally RCP2.6, RCP4.5, RCP6.0, and RCP8.5—are labelled after a possible range of radiative forcing values in the year 2100 2.6, 4.5, 6, and 8.5 W/m2, respectively (Moss et al. 2008; van Vuuren 2011; Weyant et al. 2009).

The RCP2.6 scenario was included in the RCP set to show what it would take to limit globally averaged warming to about 1 °C by 2100. RCP2.6 is generally not used in presenting plausible futures because it requires such extreme mitigation that it is considered by many climate experts to be unrealistic. The RCP2.6 scenario required that after 2020, CO_2 emissions would decline and become negative by 2100 (i.e., we find ways to sequester more carbon than we are emitting in 2100). Given the present increase in the rate of emissions and CO_2 concentrations, a near-term stabilization and decrease of emissions is not plausible.

Table 2. Two Global Climate Models (GCM) and a composite of five-model averaged GSMs scaled down to 1 by 1 km spatial resolution across Alaska used for permafrost dynamics simulation.

Project	Center	Model	Acronym
CMIP5/ AR5	National Center for Atmospheric Research	Community Earth System Model 4	NCAR-CCSM4
CMIP5/ AR5	NOAA Geophysical Fluid Dynamics Laboratory	Coupled Model 3.0	GFDL-CM3
CMIP5/ AR5	5-model averaged	Calculated as the mean of the 5 models	5-model average

6 Sensitivity Analysis

Uncertainties in the presented model lie in specifying the thermal parameters such as heat capacity of frozen and thawed soils and thermal conductivity. But mostly uncertainties are affected by thermal conductivity and the volumetric soil moisture content. The employed values for the soil properties are recovered by assimilating in situ temperature observations at a series of the Geophysical Institute, UAF and USGS sites across Alaska. The model is verified by comparing with available active layer thickness at the Circumpolar Active Layer Monitoring (CALM) sites, permafrost temperature, and snow depth records from existing permafrost observatories in Alaska. All of these datasets may contain some biases and errors. To gain some knowledge about how they act together and influence the results, we conduct a sensitivity analysis for a typical permafrost observing station at the region of discontinuous permafrost distribution. For a few other locations within continuous and sporadic permafrost regions, we obtained similar results.

For the Livengood station, a station with a typical natural condition at the interior Alaska, we analyze sensitivity of the mean annual ground temperature (MAGT) at 1 m depth and active layer thickness (ALT) with respect to the volumetric soil moisture content, thermal conductivity of thawed and frozen soils (Figure 4) and surface conditions. Our previous investigations shown that variations in the heat capacity frozen and thawed soils do not significantly affect the modeling results for ALT and MAGT (Marchenko 2008; Nicolsky et al. 2009; Wang 2012; Huang et al. 2014; Hirota et al. 2002). The obtained sensitivity results for thermal conductivity are shown in Figure 4. As the MAGT increased, the ALT increased also.

The most influence on the mean ALT and MAGT is imposed by the values of thermal conductivity of thawed soils (Figure 4). The most impact on the MAGT is imposed by the values of thermal conductivity of thawed and frozen soils for the first 0.25 m in depth and soil layers between 0.1 m and 1 m in depth. The value of frozen conductivity affects the soil layer below 1 m, and soil water content for the layer between 0.1 and 1.0 m depth. Values of the thermal conductivity for the upper layers is a primary function of the organic matter content and soil moisture. It is probable that for the future long-term projections modeling runs it is necessary to incorporate a module of organic matter accumulation dynamics into the GIPL2-MPI model.

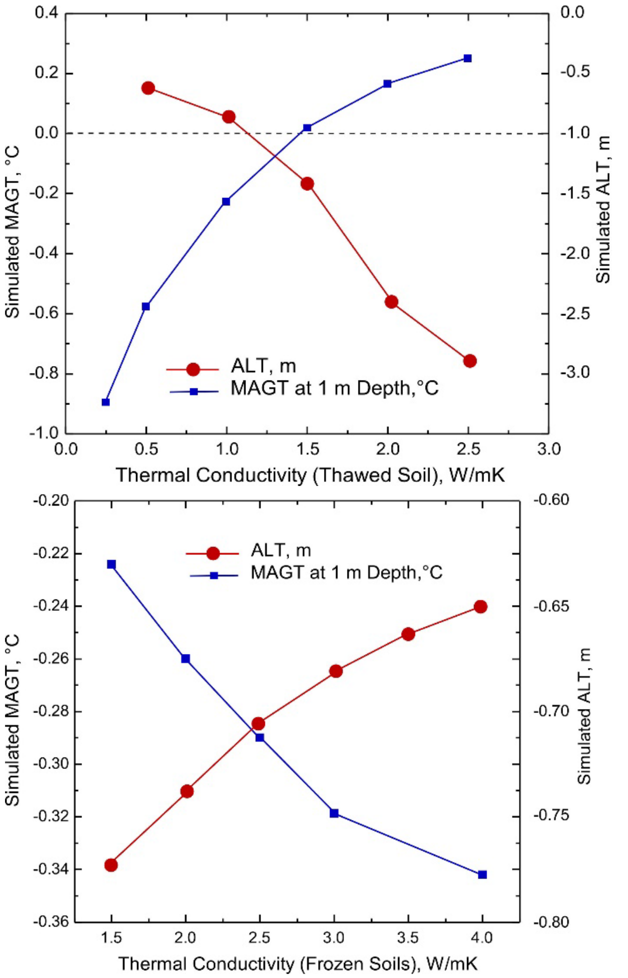

Figure 4. The sensitivity of the modeled MAGT at 1 m depth averaged for 1995–2020 (blue line with rectangles) and averaged ALT for the same period (red line with rounds) on changes in the thermal conductivity for the thawed and frozen materials for each soil layer for the Livengood Station.

7 Discussion

The developed model allows computations of the MAGT at different depths, ALT, and talik thickness projections into the future for various climate scenarios. In this research, we demonstrate the projections for two GCMs and five-model average only for RCP4.5 and RCP8.5 scenarios and illustrate a drastic difference in the future near-surface ground temperature regimes in 2070s and 2110s. For the RCP8.5 scenario, we found that ALT or top of permafrost deepening, up to 1.5 m on average in 2021, increases by a factor of 2.5 by 2070 and by a factor 3.5 from 2070 to 2120, according to the GFDL-CM3 RCP8.5 scenario. ALT continues to increase and widespread taliks starts to develop in interior Alaska and even at the North Slope region. According to NCAR-CCSM4 RCP8.5 scenario the factor of permafrost top deepening increased by 1.8 from 2021 to 2070 and by the factor of 3.2 from 2070 to 2120. Development of talik will have serious implications for ecosystems, human activities (infrastructure and subsistence lifestyle), and potential feedback to climate change. On the other hand, for the RCP4.5 scenario, the current model predicts only a modest increase in the near-surface permafrost temperatures and a limited degradation of the near-surface permafrost in the Alaska North Slope region. Finally, we mention that according to our computer experiments, to keep permafrost from the substantial thawing, the RCP4.5 scenario most likely needs to be a target for the greenhouse gas emissions.

8 Conclusions

As shown in the modeling result, the most significant changes in the upper layer (0.25–5.0 m) of ground temperature, active layer thickness as well as talik development, occurred under the climate scenario provided by the GFDL-CM3 climate model both 4.5 and 8.5 RCPs. As described by the IPCC the RCP4.5 is an intermediate scenario. Increase in soil temperature in RCP4.5 peaks around 2051–2070, then observed relative decline. RCP4.5 is more likely than not to result in global temperature rise between 2.5 °C and 3.5 °C, by 2120. In RCP8.5, ground temperature continues to rise throughout the 21st century.

The GFDL-CM3 provides more aggressive climate change scenario in comparison with NCAR-CCSM4 climate model. Under the same ecosystem conditions, the greatest changes in permafrost occur according to the GFDL-CM3, mostly under RCP-8.5 scenario.

9 Acknowledgements

This project funded under the Department of Defense (DoD), U.S. Army Engineer Research and Development Center (ERDC), the Cold Regions Research and Engineering Laboratory (CRREL) under Contract No. W913E521C0010. The GIPL2-MPI/GCM simulations were supported in part by the high-performance computing and data storage resources operated by the Research Computing Systems Group at the University of Alaska Fairbanks Geophysical Institute.

10 References

Alifanov, O. 1994. *Inverse Heat Transfer Problems*. Springer, Berlin.

Alifanov, O., Artyukhin, E., and Rumyantsev, S. 1996. *Extreme Methods for Solving Ill-Posed Problems with Application to Inverse Heat Transfer Problems*. New York, New York, United States: Begell House.

Biskaborn, B.K., Smith, S.L., Noetzli, J. et al. 2019. ‘Permafrost is warming at a global scale’, *Nature Communication* 10, 264(2019). Available at: https://doi.org/10.1038/s41467-018-08240-4.

Fiddes, J., Endrizzi, S., and Gruber, S. 2015. ‘Large-area land surface simulations in heterogeneous terrain driven by global data sets: Application to mountain permafrost’, *Cryosphere* 9, pp. 411–426.

Gisnås, K., Etzelmüller, B., Farbrot, H., Schuler, T., and Westermann, H. 2013. ‘CryoGRID 1.0: Permafrost distribution in Norway estimated by a spatial numerical model’, *Permafrost Periglacial Processes* 24, pp. 2–19.

He, Y., Genet, H., McGuire, A.D., Zhuang, Q., Wylie, B.K., and Zhang, Y. 2016. ‘Terrestrial carbon modeling - Baseline and projections in lowland ecosystems of Alaska’, in Z. Zhu and A.D. McGuire (eds.), *Baseline and projected future carbon storage and greenhouse-gas fluxes in ecosystems of Alaska*. U.S. Geological Survey Professional Paper 1826, pp. 133–158. Available at: https://doi.org/10.3133/pp1826.

Hirota, T., Pomeroy, J.W., Granger, R.J. and Maule, C.P. 2002. ‘An extension of the force-restore method to estimating soil temperature at depth and evaluation for frozen soils under snow’, *Journal of Geophysical Research* 107, pp. 4767.

Huang, F., Zhan, F., Ju, W., and Wang, Z. 2014. ‚Improved reconstruction of soil thermal field using two-depth measurements of soil temperature’, *Journal of Hydrology* 519, Part A, pp. 711–719.

IPCC 2014. ‘Climate Change 2014: Synthesis Report’, in R.K. Pachauri and L.A. Meyer (eds.) *Fifth Assessment Report of the Intergovernmental Panel on Climate Change*. Geneva, Switzerland: Contribution of Working Groups I, II and III, 151 pp.

Jafarov, E., Marchenko, S., and Romanovsky, V.E. 2012. ‘Numerical Modeling of Permafrost Dynamics in Alaska Using a High Spatial Resolution Dataset’, *The Cryosphere* 6, pp. 613–624.

Jorgenson, T., Yoshikawa, K., Kanevskiy, M., Shur, Y., Romanovsky, V., Marchenko, S., Grosse, G., Brown, J., and Jones, B. 2008. ‘Permafrost Characteristics of Alaska’, in D. Kane and K. Hinkel (eds.), *Ninth International Conference on Permafrost*. Fairbanks, Alaska, United States: June 29–July 3, 2008, pp. 121–122.

Marchenko, S.S. and Gorbunov, A.P. 1997. ‘Permafrost Changes in the Northern Tien Shan Mountains during the Holocene’, *Permafrost and Periglacial Processes* 8, pp. 427–435.

Marchenko, S., Romanovsky, V., and Tipenko, G. 2008. ‘Numerical Modeling of Spatial Permafrost Dynamics in Alaska’, in D. Kane and K. Hinkel (eds.), *Proceedings of the Ninth International Conference on Permafrost*. Fairbanks, Alaska, United States: June 29–July 3, 2008, pp. 1125–1130.

Moss, R.H., et al. 2008. *Towards New Scenarios for Analysis of Emissions, Climate Change, Impacts, and Response Strategies*. Geneva, Switzerland: Intergovernmental Panel on Climate Change, 132 pp.

Nicolsky, D., Romanovsky, V., and Panteleev, G.G. 2009. ‘Estimation of soil thermal properties using in-situ temperature measurements in the active layer and permafrost’, *Cold Regions Science and Technology* 55, pp. 120–129.

Osterkamp, T.E. and Jorgenson, J.C. 2006. ‘Warming of Permafrost in the Arctic National Wildlife Refuge', Alaska’, *Permafrost and Periglacial Processes* 17, pp. 65–69. doi:10.1002/ppp.538.

Osterkamp, T.E. (2007). ‘Characteristics of the recent warming of permafrost in Alaska’, *Journal of Geophysical Research* 112(F2): F02S02. doi:10.1029/2006JF000578.

Osterkamp, T.E. 2005. ‘The recent warming of permafrost in Alaska’, *Global and Planetary Change* 49, pp. 187–202.

Osterkamp, T.E. 2008. ‘Thermal state of permafrost in Alaska during the fourth quarter of the twentieth century’, in D. Kane and K. Hinkel (eds.) *Proceedings of the Ninth International Conference on Permafrost*. Fairbanks, Alaska, United States: June 29–July 3, 2008, pp. 1333–1338.

Romanovsky, V.E., Marchenko, S.S., Daanen, R., Sergeev, D.O., and Walker, D.A. 2008. ‘Soil Climate and Frost Heave Along the Permafrost/Ecological North American Arctic Transect’, in D. Kane and K. Hinkel (eds.) *Proceedings of the Ninth International Conference on Permafrost*. Fairbanks, Alaska, United States: June 29–July 3, 2008, pp. 1519–1524.

Romanovsky, V.E., Smith, S.L., and Christiansen, H.H. 2010. ‘Permafrost Thermal State in the Polar Northern Hemisphere during the International Polar Year 2007–2009: a Synthesis’, *Permafrost and Periglacial Processes* 21, pp. 106–116. doi:10.1002/ppp.689.

Shur Y.L. and Jorgenson M.T. 2007. ‘Patterns of permafrost formation and degradation in relation to climate and ecosystems’, *Permafrost and Periglacial Processes* 18, pp. 7-19.

Smith, S., Romanovsky, V., Lewkowicz, A., Burn, C., Allard, M., Clow, G., Yoshikawa, K., and Throop, J. 2010. ‘Thermal state of permafrost in North America: A contribution to the International Polar Year’, *Permafrost Periglacial Processes* 21, pp. 117–135.

Tikhonov, L. and Leonov, A. 1996. *Nonlinear Ill-posed Problems. Vol. 14 of Applied Mathematics and Mathematical Computation Series*. London: Chapman and Hall.

van Vuuren, D.P., Edmonds, J., Kainuma, M. et al. 2011. ‘The representative concentration pathways: an overview’, *Climatic Change* 109(5). Available at: https://doi.org/10.1007/s10584-011-0148-z.

Wang, Z.H. 2012. ‘Reconstruction of soil thermal field from a single depth measurement’, *Journal of Hydrology* 464–465, pp. 541–549.

Westermann, S., Schuler, T., Gisnås, K., and Etzelmüller, B. 2013. ‘Transient thermal modeling of permafrost conditions in southern Norway’, *Cryosphere* 7, pp. 719–739.

Weyant, J., Azar, C., Kainuma, M., Kejun, J., Nakicenovic, N., Shukla, P.R., La Rovere, E., and Yohe, G. 2009. *Report of 2.6 Versus 2.9 Watts/m2 RCPP Evaluation Panel (PDF)*. Geneva, Switzerland: IPCC Secretariat.

Zhang, Y., Wang, X., Fraser, R., Olthof, I., Chen, W., Mclennan, D., Ponomarenko, S., and Wu, W. 2013. ‘Modelling and mapping climate change impacts on permafrost at high spatial resolution for an Arctic region with complex terrain’, *Cryosphere* 7, pp. 1121–1137.

Appendix A. Result of the GIPL2-MPI Spatial and Temporal Permafrost Dynamics Modeling.

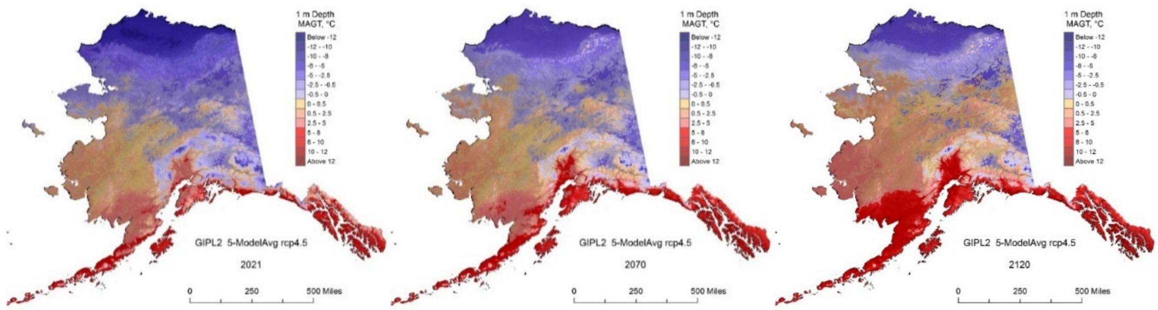

A B C

Figure 5. The GIPL2-MPI modeled mean annual ground temperature at 1 m depth for 2021 (A), 2070 (B) and 2120 (C) using five-model average RCP4.5 as a climate forcing.

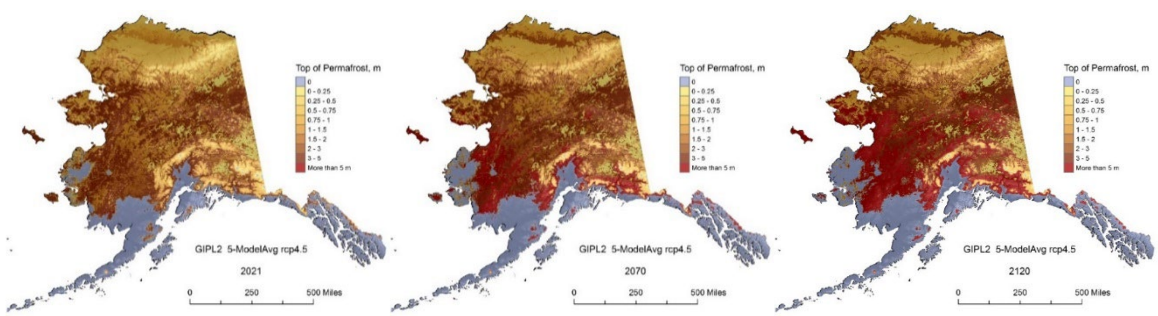

A B C

Figure 6. The GIPL2-MPI modeled top of permafrost (permafrost table) position for 2021 (A), 2070 (B) and 2120 (C) using five-model average RCP4.5 as a climate forcing.

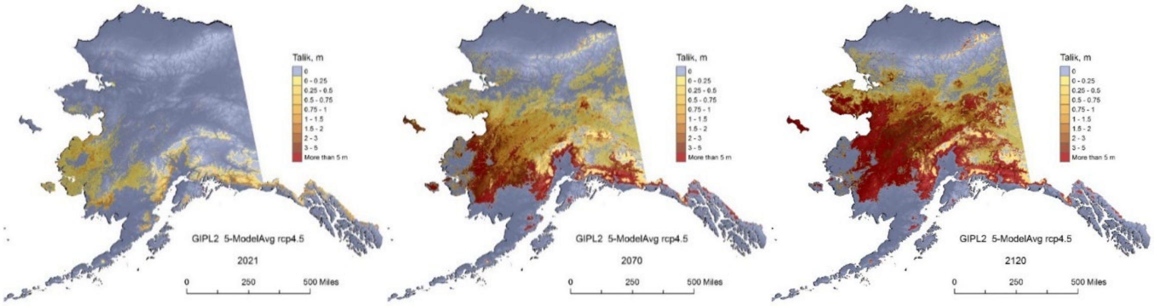

A B C

Figure 7. The GIPL2-MPI modeled Talik thickness for 2021 (A), 2070 (B) and 2120 (C) using five-model average RCP4.5 as a climate forcing.

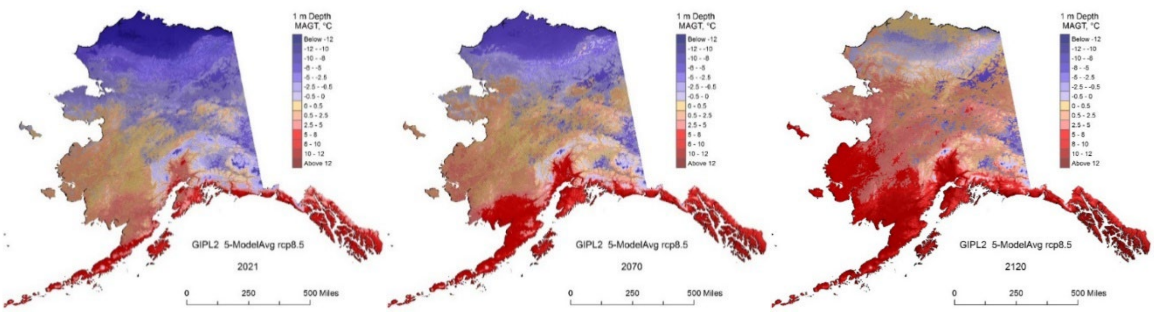

A B C

Figure 8. The GIPL2-MPI modeled mean annual ground temperature at 1 m depth for 2021 (A), 2070 (B) and 2120 (C) using five-model average RCP8.5 as a climate forcing.

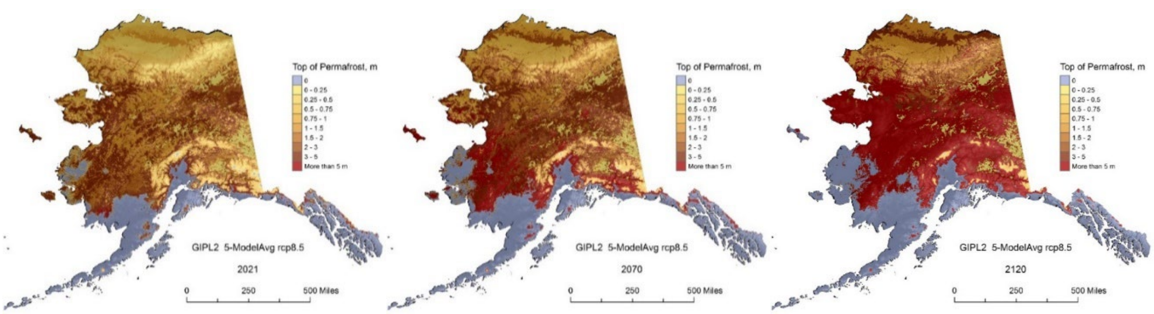

A B C

Figure 9. The GIPL2-MPI modeled top of permafrost (permafrost table) position for 2021 (A), 2070 (B) and 2120 (C) using five-model average RCP8.5 as a climate forcing.

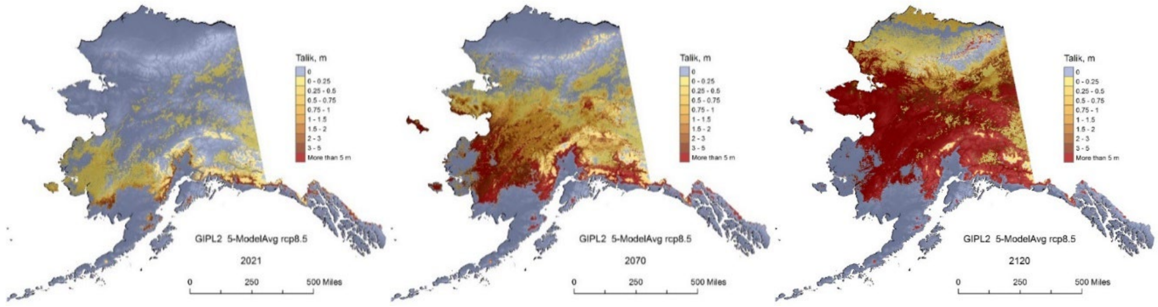

A B C

Figure 10. The GIPL2-MPI modeled Talik thickness for 2021 (A), 2070 (B) and 2120 (C) using five-model average RCP8.5 as a climate forcing.